Universität Potsdam

A.V. Runov, M.I. Pudovkin, Claudia-Veronika Meister

The dynamics of tail-like current sheets under the influence of small-scale plasma turbulence

NLD Preprints ; 54

The dynamics of tail-like current sheets under the influence of small-scale plasma turbulence

A.V. Runov[1], **M.I. Pudovkin**[1] **and C.-V. Meister**[2]

[1]Saint-Petersburg University, Russia
[2]Astrophysical Institute Potsdam, Germany

Received: June 1999

Abstract. A 2D-magnetohydrodynamic model of current-sheet dynamics caused by anomalous electrical resistivity as result of small-scale plasma turbulence is proposed. The anomalous resistivity is assumed to be proportional to the square of the gradient of the magnetic pressure as may be valid for instance in the case of lower-hybrid-drift turbulence. The initial resistivity pulse is given. Then the temporal and spatial evolution of the magnetic and electric fields, plasma density, pressure, convection and resistivity are considered. The motion of the induced electric field is discussed as indicator of the plasma disturbances. The obtained results found using much improved numerical methods show a magnetic field evolution with x-line formation and plasma acceleration. Besides, in the current sheet, three types of magnetohydrodynamic waves occur, fast magnetoacoustic waves of compression and rarefaction as well as slow magnetoacoustic waves.

Introduction

In space physics, current sheets, separating two plasma regions which have antiparallel magnetic field components, seem to play a key role. According to the terminology of Alfvén (Alfvén, 1981), current sheets are physical active regions, the (as a rule, small-scale) processes in which determine the situation in the ambient physical passive space. In this paper, the dynamics of tail-like current sheets is considered which possess additionally a small normal component of the magnetic field (Lee et al, 1994; Lin and Lee, 1994). Tail-like configurations occur for instance in planetary magnetospheres, stellar magnetic active regions and in current sheets of stellar plasma winds. It is assumed that relating to the rapid burst-like dynamics of such field configurations characteristics of stellar flares, of planetary magnetic storms and the plasmoid formation in the interplanetary medium can be explained.

During the last thirty years it became clear, that the dynamical behaviour of current sheets strongly depends on the local decrease of the effective electrical conductivity in a relatively small region of the sheets, the so-called diffusion region. According to recent opinions, the effective conductivity decrease in a current sheet may be caused by plasma turbulization, that means by the excitation of plasma waves as result of some kind of plasma instability. The waves then interact with the plasma particles, and the collision frequencies of the particles increase. The corresponding additional resistivity is called "anomalous resistivity".

The anomalous resistivity in the current sheet results in a local destruction of the current associated with a restructuring of the large-scale magnetic field, and thus causes a vortex electric field. During the local destruction of the current sheet energy stored in the magnetic field is burst-likely transformed into kinetic energy and heat. This, for instance, seems to be the cause for such events as magnetospheric substorms and stellar flares.

A simple description of current sheet destructions in the earth's magnetotail neglecting small normal components was already given by Dungey in 1961. Dungey proposed, that a so-called x-line forms in the region of decreased conductivity. According to his model the plasma in the destruction region can be accelerated up to the Alfvén velocity. The simple Dungey model was investigated in detail by Petschek (1964) and is now known as Petschek model of magnetic field line reconnection. There is a set of analytical (see e.g. (Pudovkin and Semenov, 1985) and the reviews by Rijnbeek and Semenov (1993) and Parker (1994)) and numerical (see (Hautz and Scholer, 1987; Scholer 1990)) solutions of the Petschek reconnection problem describing the plasma motion in the vicinity of the magnetic x-line.

But the process of the x-line formation itself - the earliest phase of the reconnection process - is still not well understood. The investigation of the turbulization process, theoretically as well as experimentally, is very difficult. The turbulence theory is far from being completed, and it is usually very hard to say which kind of plasma instability may develop in real situations, for example, in the magnetotail or in stellar flares (Coroniti, 1985; Liperovsky and Pudovkin, 1983; Schindler 1987; Büchner et al., 1988; Parker 1994). Besides, in the models the feedback of the large-scale electromagnetic and hydrodynamic processes on the small-scale plasma processes has to be taken into account.

In tail-like current sheets strong currents and drifts as well as magnetic stresses and plasma anisotropies can cause microturbulence. It was concluded that the two most relevant instabilities for which a steady state anomalous resistivity can be achieved in almost collisionless plasmas are the ion-acoustic (IA) and the lower-hybrid-drift (LHD) instabilities (Huba et al., 1977; Hoshino, 1991). But in the case of the IA instability, the relative electron-ion drift must be much larger than $v_e\sqrt{T_i/T_e}$, which is seldom the case, and dissipation may only occur in very thin diffusion sheets of a thickness of $\delta < c/\omega_{pe}$ (Coroniti, 1985) (T_e, T_i, v_e, ω_{pe}, c are electron and ion temperature, electron thermal velocity, electron plasma frequency and velocity of the light in vacuum). On the contrary, the LHD instability can be very effective under the condition $T_i > T_e$ too, but it also causes a small diffusion region of the dimension of the ion Larmor radius only, $20c/\omega_{pe} \leq \delta \leq (m_i/m_e)^{1/4} r_{Li}$ (Coroniti, 1985). In the earth's magnetotail LHD waves were indeed observed by ISEE satellites as low-frequency part of broadband electrostatic noise.

Beginning with Ugai and Tsuda (1977), the evolution of current sheets was investigated assuming localized anomalous resistivity profiles with a peak at the neutral sheet. Hoshino (1991) first considered anomalous resistivity caused by LHD turbulence out of the neutral line. But he did not take into account a small normal component of the magnetic field.

Thus, here it is assumed that the current density in a local region at the symmetry plane of a tail-like current sheet exceeds the threshold of some current-driven plasma instability. It may be, for example, the electrostatic ion-cyclotron (EIC) instability in the magnetotail, or the ion-acoustic (IA) instability in solar flares (see Kindel and Kennel, 1971; Galeev and Sagdeev, 1973; Liperovsky and Pudovkin, 1983). The instability gives rise to a rapid decrease of the electrical conductivity of the plasma in the centre of the current sheet, which initiates the development of a magnetic reconnection pulse. This, in turn, results in a generation of relatively intensive magnetohydrodynamic waves with secondary pressure gradients at their fronts, and then it may be supposed that the LHD instability is excited by those pressure gradients.

This instability occurs if the scale of the magnetic field gradient L_B is smaller or of the order of seven ion Larmor radii. This means, for instance, for the tail of the earth's magnetosphere that secondary current sheets with maximum widths of approximately 2100-2800 km and diffusion regions with maximum thicknesses of about 1000-1500 km should exist. Correspondingly, the minimum thickness of the plasma sheet which has to contain at least two secondary diffusion regions is about 2000-3000 km. These values are in reasonable agreement with the thicknesses of current sheets in the plasma sheet during growth phases of substorms of about 3000 km given in (Sergeev et al. 1990). In this case, the used magnetohydrodynamic approach is applicable as the condition $L_B > r_{Li}$ is fulfilled, and the Debye radius is of the order of 0.3-0.4 km.

Besides, in the last years, it was also shown by Pulkkinen (1992; 1994) that rather thin (500-1000 km) and relatively intense (1-20 mA/m) current sheets develop in the near-earth magnetotail during substorm growth phases. The thin current sheets were accompanied by small normal components B_n of the magnetic field. For these current sheets, one has $L_B \sim 1-2\ r_{Li}$, and the magnetohydrodynamic approach is not valid.

Thus, we consider the development of a tail-like current sheet under the influence of both, a strong initial resistivity pulse at the neutral sheet and anomalous resistivity caused by LHD-turbulence. The main attention is paid to the behaviour of the electric field in the diffusion region and nearby, especially during the earliest phase of the reconnection process.

Model of the Current Sheet

It is assumed that the plasma of the tail-like current sheet is described by the compressible magnetohydrodynamic equations (Hoshino, 1991)

$$\frac{\partial}{\partial t}\rho = -\nabla \cdot (\rho \mathbf{v}), \tag{1}$$

$$\rho(\frac{\partial}{\partial t}\mathbf{v} + (\mathbf{v}\cdot\nabla)\mathbf{v}) = -\nabla p + (\nabla \times \mathbf{B}) \times \mathbf{B}, \tag{2}$$

$$\frac{\partial}{\partial t}\mathbf{A} = \mathbf{v} \times (\nabla \times \mathbf{A}) + \frac{1}{Re_m}\nabla^2 \mathbf{A}, \tag{3}$$

$$\frac{\partial}{\partial t}p = -\nabla \cdot (p\mathbf{v}) + (\gamma - 1)(-p\nabla \cdot \mathbf{v} + \frac{1}{Re_m}(\nabla \times \mathbf{B})^2), \tag{4}$$

$$\mathbf{B} = \nabla \times \mathbf{A}, \tag{5}$$

$$\nabla \cdot \mathbf{A} = 0, \tag{6}$$

where ρ, p and $\mathbf{v}$ are the plasma density, pressure and velocity normalized by the characteristic values ρ_0, p_0, v_a of the undisturbed plasma. $\mathbf{B}$ designates the magnetic field normalized by the value B_0 of the current sheet environment at $z \gg \delta$, and $\mathbf{A}$ is the magnetic vector-potential. The x-axis is assumed to be directed along the current sheet, so that the electric current flows in y-direction. δ describes the half-thickness of the sheet in z-direction. $Re_m = 4\pi\sigma v_a L/c^2$ is the magnetic Reynolds number of a plasma with characteristic length L and characteristic velocity of the order of the Alfvén velocity $v_a = B_0/\sqrt{4\pi\rho_0}$. The temporal variable is normalized by the specific Alfvén transport time $t_a = L/v_a$, γ is the ratio of the specific heats, $\gamma = c_p/c_V$, and σ designates the electrical conductivity. The hydrodynamic viscosity is neglected in the model, and the plasma pressure is assumed to be isotropic.

The initial tail-like plasma configuration is described by the solution of the Grad-Shafranov equation

$$A(x,z) = -\delta \ln \left(\frac{\cosh(f(x)z/\delta)}{f(x)} \right), \tag{7}$$

$$f(x) = (1+kx)^{\alpha}, \;\; \alpha < 0, \tag{8}$$

$$p(x,z) = \frac{\delta}{2} \frac{f(x)^2}{\cosh^2(f(x)z/\delta)}, \tag{9}$$

(see (Hau et al., 1989; Pritchett et al., 1991; Hesse et al., 1996)).

The resistivity is supposed to have the form

$$\eta(x,z,t) = \eta_l + \eta^* + \eta_0 \tag{10}$$

(Runov et al., 1998), where η_0 is the background resistivity, which is of the order of the numerical resistivity of the meshgrid. The first term on the right-hand side of Eq. (10)

$$\eta_l(x,z,t) = \begin{cases} \eta_m \exp\{-(a^2x^2+b^2z^2)/2\}(1-\exp\{t/t_i\}), & \text{if } t \le t_c \\ \eta_l(x,z,t_c)\exp\{(t-t_c)/t_r\}, & \text{if } t > t_c \end{cases} \tag{11}$$

represents the initial pulse of anomalous resistivity, introduced to start up a local current sheet destruction. t_i is the characteristic time of the initial resistivity growth, t_c gives the resistivity pulse duration, and t_r is the relaxation time of the resistivity pulse, $a^{-2} \approx b^{-2} \approx 0.1\ L$. The temporal variation of η_l with $t_i = t_r = 0.025t_a$, and $t_c = 0.25t_a$, used in the calculations, is shown in Fig. 1. Finally,

$$\eta^*(x,z,t) = \begin{cases} \eta^*_m(\nabla B^2(x,z,t) - \nabla B^2(x,z,t_0))^2, & \text{if } \nabla B^2(x,z,t) - \nabla B^2(x,z,t_0) > 0 \\ 0, & \text{otherwise} \end{cases} \tag{12}$$

represents the plasma resistivity within the regions of the secondary pressure gradients produced in the course of the plasma sheet evolution, and hence it describes the feedback between the resistivity and the MHD evolution of the system. η^* may be considered as the model specification.

It is assumed that η^* is caused by the LHD-instability which is driven by diamagnetic currents associated with the pressure gradient. The instability occurs if $r_{Li} < \sqrt{2}L < (m_i/m_e)^{1/4} r_{Li}$ is valid, where L is the scale of the pressure gradient which approximately equals the thickness of the current sheet. Under the condition $(m_i/m_e)^{1/4} r_{Li} < \sqrt{2}L$ the generation of ion-cyclotron drift turbulence is possible. In the high-β plasma of the magnetic neutral sheet, LHD-waves are strongly damped by the interaction with the electrons. Thus, on the contrary to the initial resistivity pulse η_l, which has a maximum at the neutral line, the anomalous resistivity η^* has its maximum relatively far from the neutral line.

In the case of rather large polarization drift velocities V_i of the ions with values above 0.18 $v_i(1 + T_e/T_i)$ (Huba et al., 1978) the LHD-instability may be damped by current relaxation processes and the effective plasma resistivity is proportional to V_i^2 (v_i, r_{Li} are the thermal velocity and the Larmor radius of the ions). V_i is proportional to the gradient of the plasma density. At $V_i > 3v_i$ saturation of the wave growth by ion trapping may occur, and the effective resistivity seems to be proportional to V_i^4. But, for instance, in the tail of the earth's magnetosphere, at a distance of 20-30 earth radii from the earth, it seems more likely that LHD-instabilities are saturated by current relaxation. Thus there, one can assume, that the electrical plasma resistivity in the turbulent region at maximum wave growth is about 10^8 Ωm, that means the resistivity may increase up to four-five orders in comparison with the plasma without turbulence (Meister 1997).

The value of η^* may be different in different models. So, Schumacher and Kliem (1997) assumed it to be proportional to the excessive current density $|j - j_{cr}|$ in linear or quadratic dependence.

In this paper, following (Hoshino, 1991), the effective resistivity in the turbulent region is supposed to be proportional to the square of the mean magnetic field gradient (Eq. (13)). Such a magnetic-field-gradient dependence was already published in (Huba et al., 1977).

Simulation Results

The system of Eqs. (1-13) is solved numerically using the two-step predictor-corrector Lax-Wendroff method (Scholer and Roth, 1987; Scholer et al., 1990) and the absolutely stable Dufort-Frankel scheme (Dautray and Lions, 1993). The both methodes are of second order of precision with respect to space and time grid steps. The computation was made in the range $1 \leq x/L \leq 10$, $0 \leq z/L \leq 1$ in uniform numerical box 100×100 meshes, with cell sizes $\Delta x/L = 0.05$, $\Delta z(z = 0)/L = 0.01$. The time step was calculated from the Courant-Friedrichs-Levy stability condition (Dautray and Lions, 1993), $\Delta t/\tau \approx 10^{-5}$.

The free boundary conditions are specified at the boundaries $x = 0$, $x = 10$, and $z = 1$. It means that mass flux, energy flux and magnetic field can freely exit the numerical box (Scholer and Roth, 1987; Hoshino, 1991). The symmetry/antysymmetry conditions are specified at the $z = 0$ boundary.

The following model parameters of the initial configuration was chosen: $\delta = 0.1L$, $k = 5.0$, $\alpha = -3.5$.

The inverse initial magnetic Reynolds number pulse (see Eqs. (11, 12)) used for the calculations is represented in the upper panel of Fig. 1 as function of time. The maximum value of η_l/η_0 equals 50 in the center of the diffusion region.

In accordance with the ideas proposed in (Pudovkin, et al., 1997), we consider the inductive electric field $\mathbf{E} = \partial\mathbf{A}/\partial t$ as the main characteristics of the current sheet evolution. In Fig. 1 the temporal variation of the inductive electric field at the center of the initial diffusion region (curve 1) and on the sheet periphery (curve 2) are shown. The field $\mathbf{E}$ is normalized by the Alfvén electric field $E_a = B_0 v_a/c$. As it follows from the calculations, the inductive electric field first rapidly increases when the local resistivity increases, and the steepness of the $E(t)$ curve is determined by the rate of the η_l-increase. Then, in spite of the fact that the η_l-value remains constant, the electric field intensity gradually decreases with a characteristic time scale equal to the diffusion time $t_d = 4\pi\sigma_s l_d^2/c^2$, where σ_s is the average of the electrical conductivity in the diffusion region, and l_d is the half-width of the current sheet. It should be emphasized that if the anomalous resistivity is varying slowly ($\omega \ll 1/t_d$), then the temporal variation of the inductive electric field is independent on the temporal behaviour of the resistivity and may be used for the estimate of the value of η_l.

In Figs. 2.1-2.3, the spatial evolution of the inductive electric field is presented. The calculations show that at the initial stage of the process, the inductive electric field is localized in the vicinity of the given anomalous resistivity region, and with the time the electric field, which gives the information on the disturbances in the plasma-magnetic field system, propagates as a wave-like object along and across the sheet. It should be noted that the electric field maxima are moving from the sheet axis to the sheet periphery (see Fig. 2.2).

At $t = 1.00\tau$ the electric field intensity in the vicinity of the x-line is very small (Fig. 2.3). At the same time, a rather intensive electric field continues to exist at the sheet periphery. In case of the earth's magnetotail, that means, that if a second resistivity pulse would occur, within a relatively short time interval, it may appear together with a background electric field in the tail lobes. This seems to be an important conclusion suggesting that during substorms in the tail, there should exist electric field pulses with characteristic time scale of 10 s, and a background electric field with smooth temporal variation forming an envelope of the pulses.

In Fig. 3 the contours of anomalous resistivity $\eta^*(x, z)$ at $t = 1.00\tau$ are shown. The maxima of the anomalous resistivity at $t = 1.00\tau$ correspond to the maxima of the inductive electric field. It should be noted that η^* develops at the periphery of the sheet, where the plasma-β is approximately unity. No anomalous resistivity occurs near the symmetry axis of the current sheet, and only secondary diffusion regions connected with the anomalous resistivity caused by LHD-type plasma turbulence exist.

The plasma convection in the vicinity of the magnetic field x-line is demonstrated in Fig. 4. The convection is quasi-hyperbolic, which is in agreement with the Petschek-type reconnection model (see (Rijnbeek and Semenov, 1993)). The two regions containing the accelerated plasma and the anomalous B_z component correspond to the so-called field reversal (FR) regions, postulated in Petschek-type models.

Fig. 5 displays the plasma density variation $\delta\rho = \rho(t + \Delta t) - \rho(t)$ at $t = 1.00\ \tau$, where δt is the time step. The figure shows, that the perturbation of the initial steady-state plasma-magnetic field configuration by the resistivity pulse in a local but finite region is followed by the generation of three types of magnetohydrodynamic wave-like disturbances. The existence of such waves was first shown numerically in (Runov and Pudovkin, 1996). Then Semenov et al. (1997) analytically found that these waves may appear. The first type is the magnetoacoustic wave of rarefaction propagating across the magnetic field. This disturbance is characterized by small amplitude negative variations of the plasma density ($\delta\rho < 0$) and the absolute value of the magnetic field ($\delta B < 0$). The second is the fast magnetoacoustic wave of compression ($\delta\rho > 0,\ \delta B > 0$), associated with the FR-region. And the third is the slow magnetoacoustic wave ($\delta\rho > 0, \delta B < 0$), corresponding to the rotation of the plasma convection vector (wave theory see (Polovin and Demutzkiy, 1987; Lin and Lee, 1994; Sturrock, 1994)).

As it follows from the calculations, the inductive electric field and therewith the information on the disturbances is carryed by the fast magnetoacoustic wave. This seems to be an important result, because the effects of the fast wave are often neglected in Petschek-type reconnections models. The maximum of anomalous resistivity is associated with the high magnetic pressure gradient in the transition region from the fast wave of compression, where the kinetic energy of plasma has the maximum, to the slow magnetoacoustic wave, where the magnetic energy has a minimum.

4 Conclusions

A very simple physical model of a tail-like current sheet with a normal component of the magnetic field was considered. Of course, real magnetospheric substorms or solar flares occur under much more complex conditions. But, nevertheless, the model allows one to formulate general conclusions, which may be useful for the analysis of spacecraft and ground based data of substorms and flares.

1. In the vicinity of the magnetic x-line, after the initial resistivity pulse onset, the electric field

at first rapidly increases up to a value of about $E_{max} \sim 0.1 E_a$, and then decreases exponentially with a characteristic time scale equal to the diffusion time. At the late phase of the reconnection pulse, the resistivity is determined only by the anomalous LHD-resistivity, the feedback on which by the macroscopic magnetic field changes was taken into account.

2. Further, it was shown that the pulse of anomalous resistivity generates a series of magnetohydrodynamic waves propagating from the x-line. The waves are: first, fast magnetoacoustic waves with synphase variations of plasma density and absolute value of the magnetic induction. Such waves propogate along the current sheet as a compression wave and across the sheet as a rarefaction wave. Second, slow magnetoacoustic waves with anticorrelation between the variations of plasma density and absolute value of the magnetic induction were found.

3. The numerical calculation showed that during reconnection processes the inductive electric field, which contains information on the disturbances in a plasma-magnetic field system, is carryed by the fast magnetoacoustic waves along and across the current sheet.

Acknowledgements

This work is supported by the Russian Foundation for Basic Research under grants N 97-05-64458 and N 99-05-04006 as well as by the organization Deutsche Forschungsgemeinschaft, grants 436 RUS 113/77 and ME 1207/7. C.-V. Meister acknowledges financial support by the project 24-04/055-1999 of the Ministerium für Wissenschaft, Forschung und Kultur des Landes Brandenburg.

References

Alfvén, H., *Cosmic Plasma,* D. Reidel Publishing Company, Dordrecht, Holland, 1981.

Büchner J., C.-V. Meister, B. Nikutovski, Reconnection and microturbulence, *ESA SP-285*, Vol. 2, 35-40, 1988.

Coroniti, F. V., Space plasma turbulent dissipation: reality or myth? *Space Sci. Rev.*, **42**, 399-410, 1985.

Dautray, R., and J.-L. Lions, *Mathematical analysis and numerical methods for science and technology,* Vol. 6, Springer-Verlag, Berlin-Heidelberg-New York, 1993.

Dungey, J. W., Interplanetary magnetic fields and the auroral zones, *Phys. Rev. Lett.*, **6**, 47-48, 1961.

Galeev, A. A., and R. Z. Sagdeev, Nonlinear plasma physics, in: Ed. M. A. Leontovich 3-145, *Problems of Plasma Theory*, Vol. 7, Atomizdat, Moscow, 1973.

Hau, L.-N., R. A. Wolf, G.-H. Voigt, and C. C. Wu, Steady state magnetic field configuration for the earth's magnetotail, *J. Geophys. Res.*, **94**, 1303-1316, 1989.

Hautz, R., and M. Scholer, Numerical simulations on the structure of plasmoids in the deep tail, *Geophys. Res. Lett.*, **14** (9), 969-972, 1987.

Hesse, M., J. Birn, D. Baker, and J. A. Slavin, MHD simulations of the transition of magnetic reconnection from closed to open field lines, *J. Geophys. Res.*, **101** (A5), 10805-10816, 1996.

Hoshino, M., Forced magnetic reconnection in a plasma sheet with localized resistivity profile excited by lower hybrid drift type instability, *J. Geophys. Res.*, **96**, 11555-11567, 1991.

Huba, J. D., N. T. Gladd, and K. Papadopoulos, The lower-hybrid-drift instability as a source of anomalous resistivity for magnetic field line reconnection, Geophys. Res. Lett., **4** (3), 125-128, 1977.

Huba, J. D., N. T. Gladd, and K. Papadopoulos, Lower-hybrid-drift wave turbulence in the distant magnetotail, J. Geophys. Res., **83**, 5217-5226, 1978.

Kindel, J. M., and C. F. Kennel, Topside current instabilities, *J. Geophys. Res.*, **76**, 3055-3078, 1971.

Lee, L. C., L. Zhang, M. Yan, H. J. Cai, G. S. Choe, A. Otto, and S.-I. Akasofu, Formation of a very thin current sheet during substorm growth phase and plasma dynamics in the recovery phase, in: Eds. J. R. Kan, J. D. Carven, and S.-I. Akasofu, 143-148, Proc. of the second Int. Conf. on Substorms, Fairbanks, Alaska, 1994.

Lin, Y., and L. C. Lee, Structure of reconnection sheets in the magnetosphere, *Space Science Reviews,* **65**, 59-179, 1994.

Liperovsky, V. A., and M. I. Pudovkin, *Anomalous resistivity and double layers in the magnetospheric plasma,* Nauka, Moscow, 1983.

Meister, C.-V., Current fluctuations in the earth's magnetosphere caused by lower-hybrid-drift turbulence, *Adv. Space Res.,* **19** (12), 1951-1954, 1997.

Parker, E. N., *Spontaneous Current Sheets in Magnetic Fields*, University Press, Oxford, 1994.

Petschek, H. E., Magnetic field annihilation, in: *AAS-NASA Symp. on the Physics of Solar Flares*, Ed. W.N. Hess, 425-437, NASA SP-50, New York, 1964.

Polovin, R. V., V. P. Demutzkiy, *Fundamentals of Magnetohydrodynamics*, Energoatomizdat, Moscow, 1987.

Pritchett, P. L., F. V. Coroniti, R. Pellat, and H. Karimbadi, Collisionless reconnection in two-dimensional magnetotail equilibria, *J. Geophys. Res., 96,* 11523-11538, 1991.

Pudovkin, M. I., A. V. Runov, and A. V. Manankova, Electric fields in the reconnection region, in: *The Solar Wind-Magnetosphere System,* Eds. H. K. Biernat, H. P. Ladreiter, S. J. Bauer, and C. J. Farrugia, 187-194, Österreichischer Akademie-Verlag, Vienna, 1997.

Pudovkin, M. I., V. S. Semenov, *Reconnection theory and interaction of solar wind with the earth's magnetosphere*, Nauka, Moscow, 1985; Magnetic field reconnection theory and the solar wind-magnetosphere interaction. A review, *Space Sci. Rev.*, **41**, 1-89, 1985.

Pulkkinen, T. I., D. N. Baker, R. J. Pellinen, J. Büchner, H. E. J. Koskinen, R. E. Lopez, R. L. Dyson, and L. A. Frank, Particle scattering and current sheet stability in the geomagnetic tail during the substorm growth phase, *J. Geophys. Res.*, **97** (A12), 19283-19297, 1992.

Pulkkinen, T. I., D. N. Baker, D. G. Mitchell, R. L. McPherron, C. Y. Huang, and L. A. Frank, Thin current sheets in the magnetotail during substorms: CDAW 6 revisited, *J. Geophys. Res.*, **99** (A4), 5793-5803, 1994.

Rijnbeek, R. P., and V. S. Semenov, Features of Petschek-type reconnection model, *Trends in Geophys. Res.,* **2**, 247-268, 1993.

Runov, A. V., and M. I. Pudovkin, Two-dimensional MHD-model of magnetic reconnection in a current sheet of finite dimensions, *Geomagnetism and Aeronomy*, **36** (3), 13-20, 1996.

Runov, A. V., M. I. Pudovkin, and C.-V. Meister, Dynamics of a current layer with nonzero normal component of the magnetic field during the development of local anomalous resistivity, *Geomagnetism and Aeronomy*, **38** (2), 51-59, 1998.

Schindler, K., Coupling of microscopic and macroscopic processes in the earth's magnetotail, *Proc. 21st ESLAB Symposium*, Bolkesjo, Norway 1987, ESA SP-275, 39-44, 1987.

Scholer, M., and D. Roth, A simulation study on reconnection and small-scale plasmoid formation, *J. Geophys. Res.,* **92** (A4), 3223-3233, 1987.

Scholer, M., T. Terasawa, and F. Jamitzky, Reconnection and fluctuations in compressible MHD: A comparison of different numerical methods, *Computer Physics Communications,* **59**, 175-184, 1990.

Schumacher, J., and B. Kliem, Coalescence of magnetic islands including anomalous resistivity, *Phys. Plasmas,* **4** (10), 3533-3543, 1997.

Sergeev, V. A., P. Tanskanen, K. Mursula, A. Korth, and R. C. Elphic, Current sheet thickness in the near-Earth plasma sheet during substorm growth phase, *J. Geophys. Res.*, **95** (A4), 3819-3828, 1990.

Semjonov, V. S., O. A. Drobysh, and M. F. Heyn, Analytical MHD-model of spontaneous reconnection in compressible plasma, in: *Problems of Geospace*, Eds. M.I. Pudovkin, B.P. Besser, W. Riedler, A.M. Lyatskaya, 169-178, Int. Conf. Problems of Geocosmos, St.-Petersburg 17.-23.6.96, Österreichischer Akademie-Verlag, Vienna, 1997.

Sturrock, P. A., *Plasma Physics*, University Press, Cambridge, 1994.

Ugai, M., and T. Tsuda, Magnetic field line reconnection by localized enhancement of resistivity. Part 1. Evolution in a compressible MHD fluid, *J. Plasma Phys.*, **17** (2), 337-356, 1977.

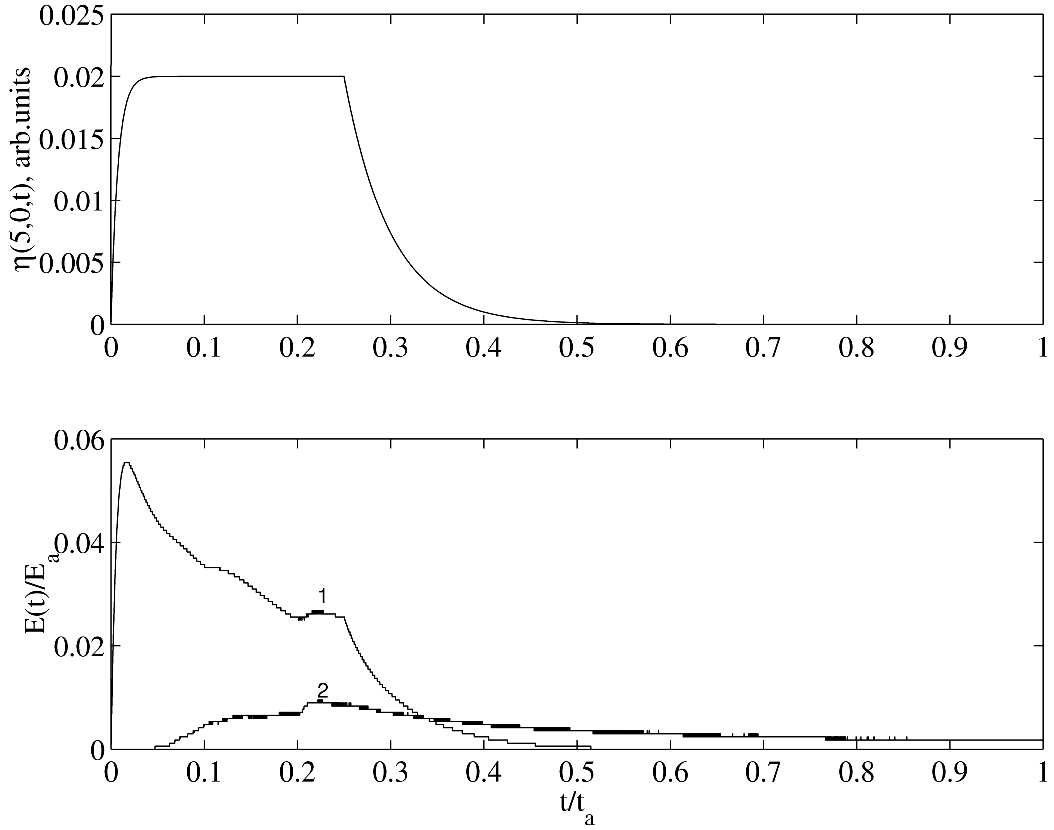

Figure 1: Inverse magnetic Reynolds number $1/Re_m$ as function of time, and temporal behaviour of the inductive electric field at the center of the initial diffusion region (curve 1) and at the periphery of the region (curve 2). $E_a = B_o v_a / c$.

Figure captions Fig. 1. Inverse magnetic Reynolds number $1/Re_m$ as function of time, and temporal behaviour of the inductive electric field at the center of the initial diffusion region (curve 1) and at the periphery of the region (curve 2). $E_a = B_o v_a / c$.

Fig. 2.1 Contours of the vector potential and inductive electric field at time $t = 0.25\tau$.

Fig. 2.2 The same as in Fig. 2.1 at $t = 0.50\tau$.

Fig. 2.3 The same as in Fig. 2.1 at $t = 1.00\tau$.

Fig. 3. Contours of the vector potential and plasma resistivity at time $t = 1.00\tau$.

Fig. 4. Contours of the vector potential and plasma velocity vectors at time $t = 1.00\tau$.

Fig. 5. Contours of the vector potential and plasma density variation at time $t = 1.00\tau$.

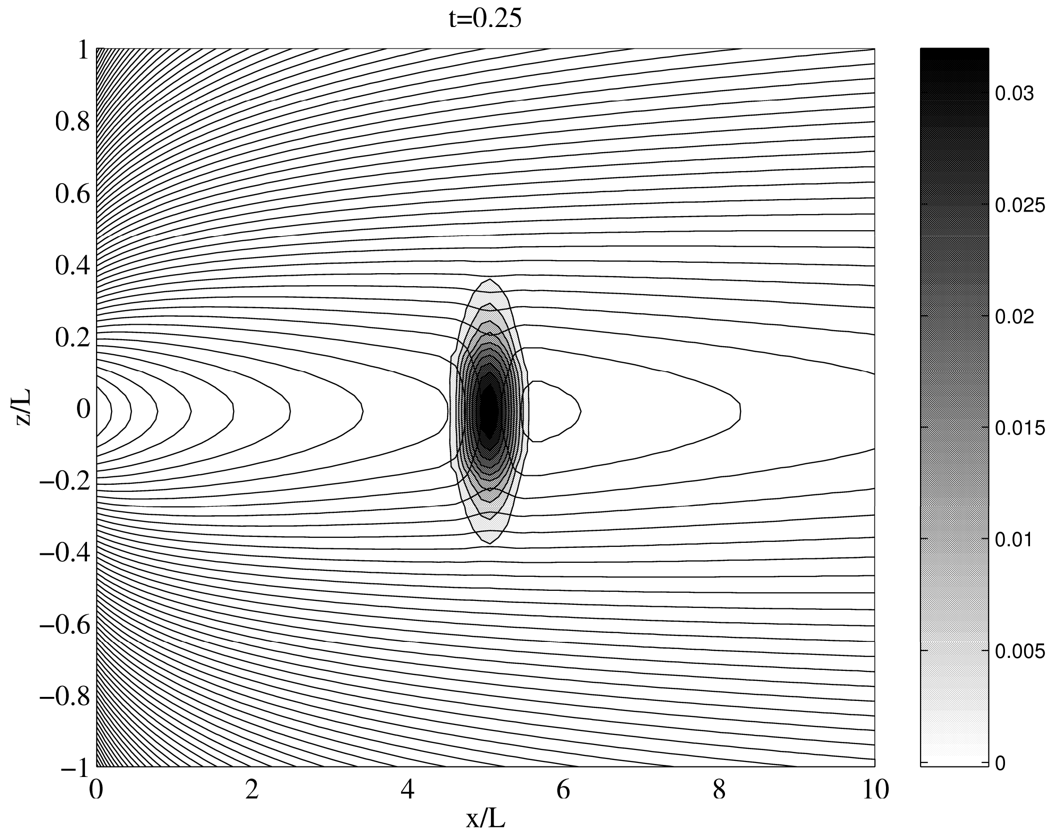

Figure 2: Contours of the vector potential and inductive electric field at time $t = 0.25\ t_a$.

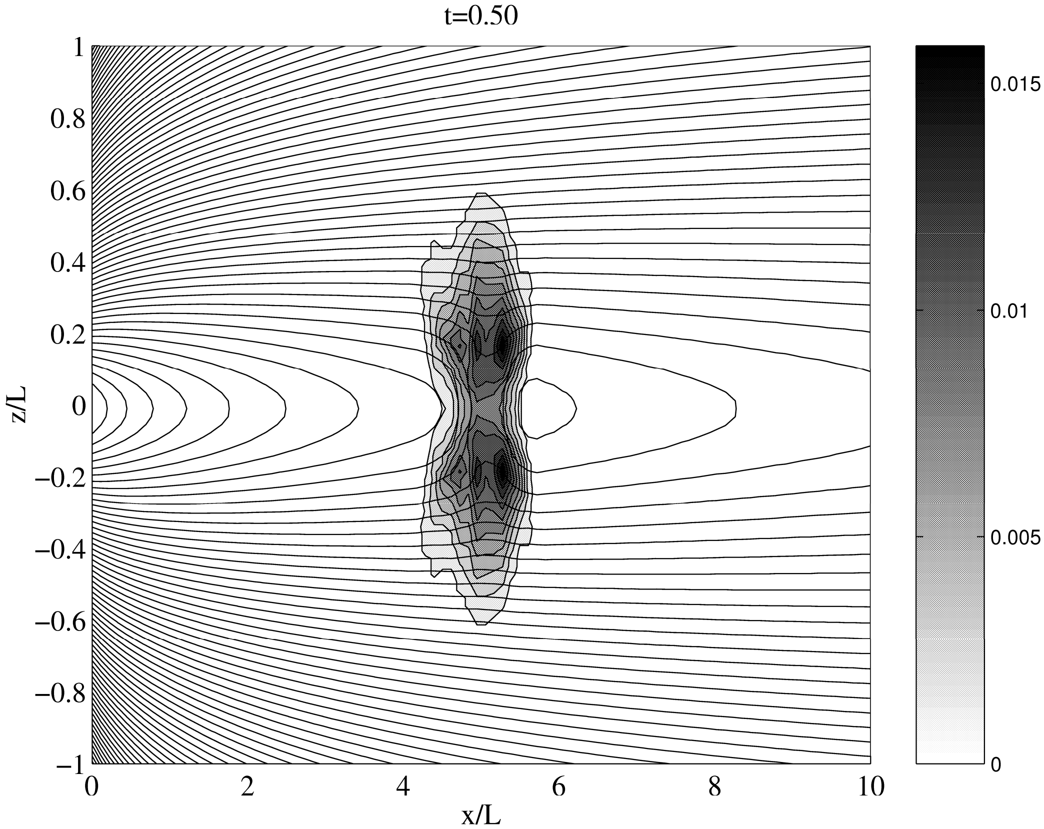

Figure 3: Contours of the vector potential and inductive electric field at time $t = 0.50\ t_a$.

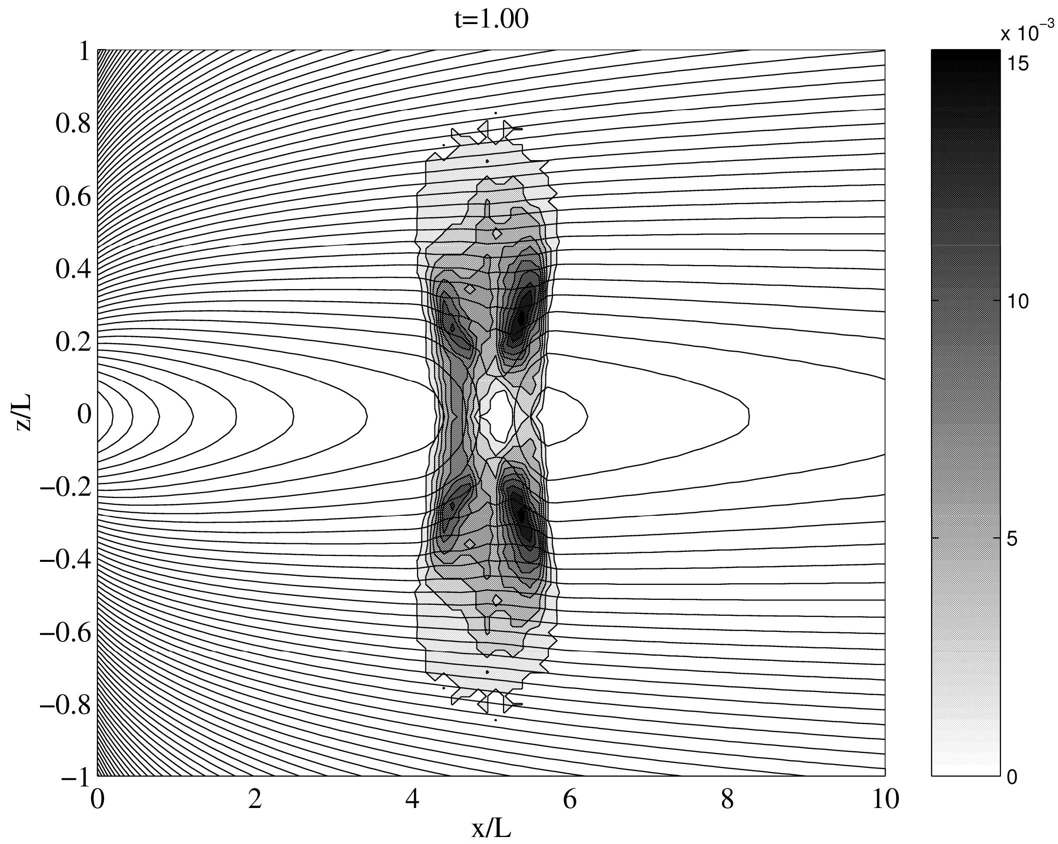

Figure 4: Contours of the vector potential and inductive electric field at time $t = 1.00\ t_a$.

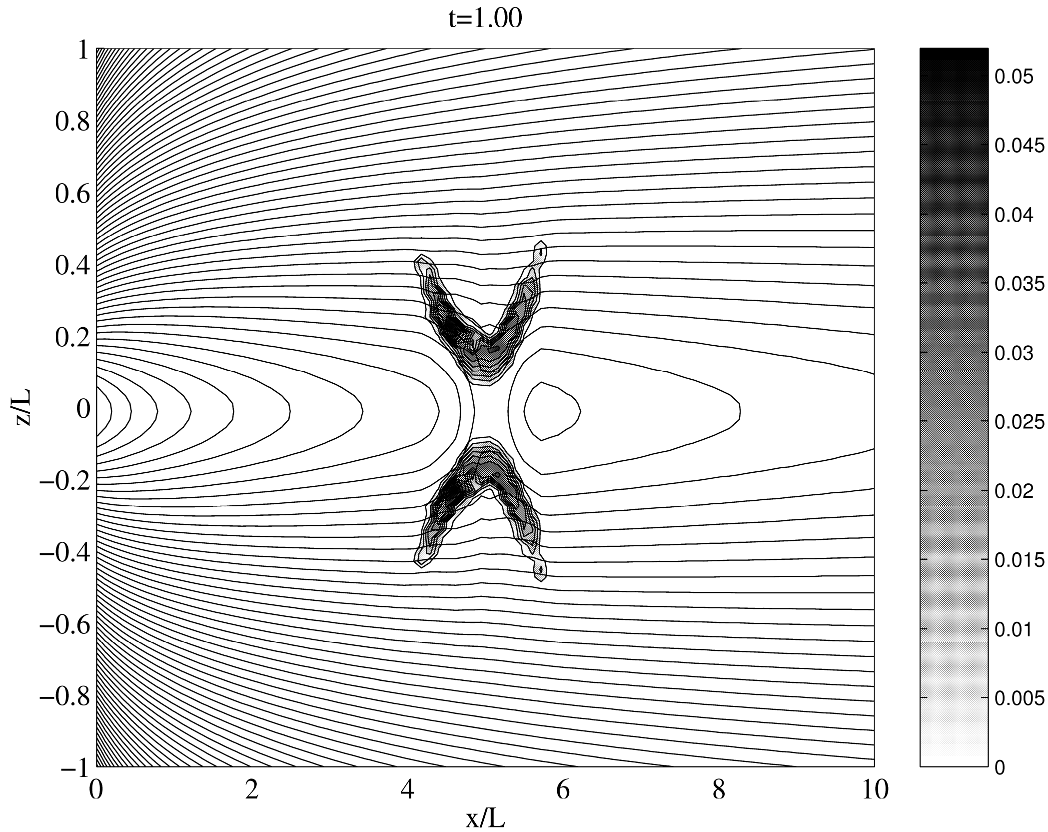

Figure 5: Contours of the vector potential and plasma resistivity at time $t = 1.00\ t_a$.

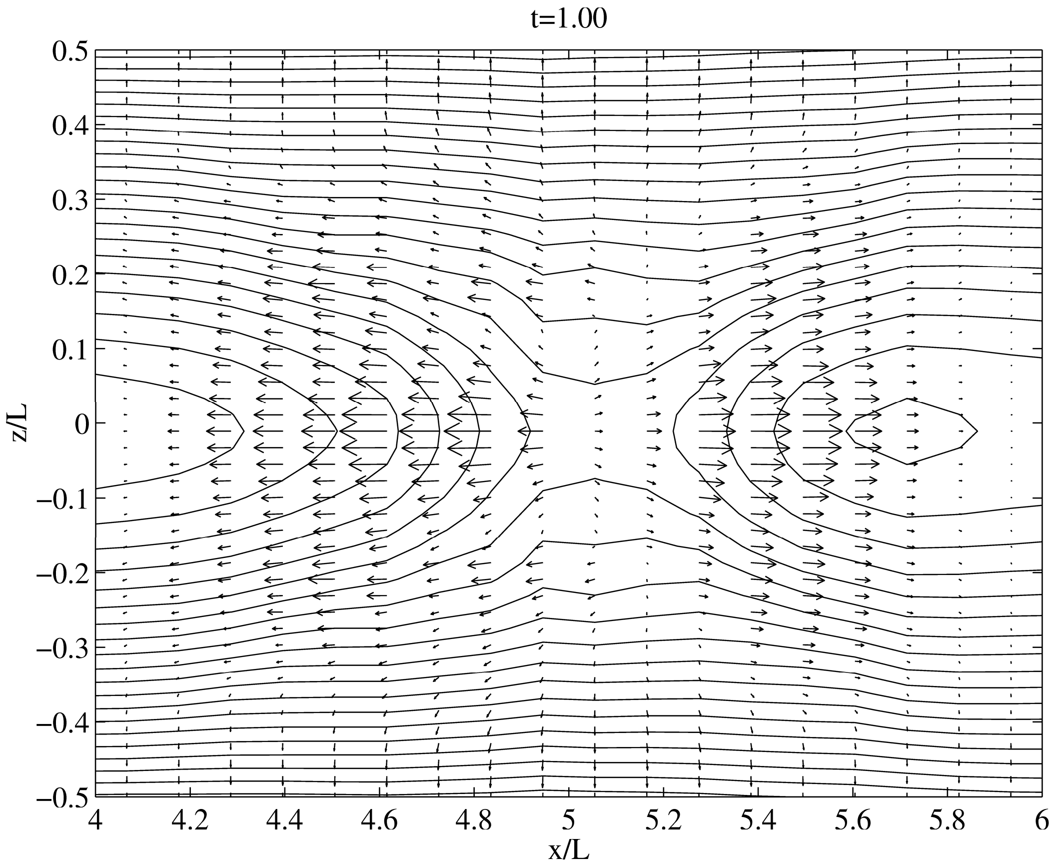

Figure 6: Contours of the vector potential and plasma velocity vectors in the vicinity of the magnetic field x-line at time $t = 1.00\ t_a$.

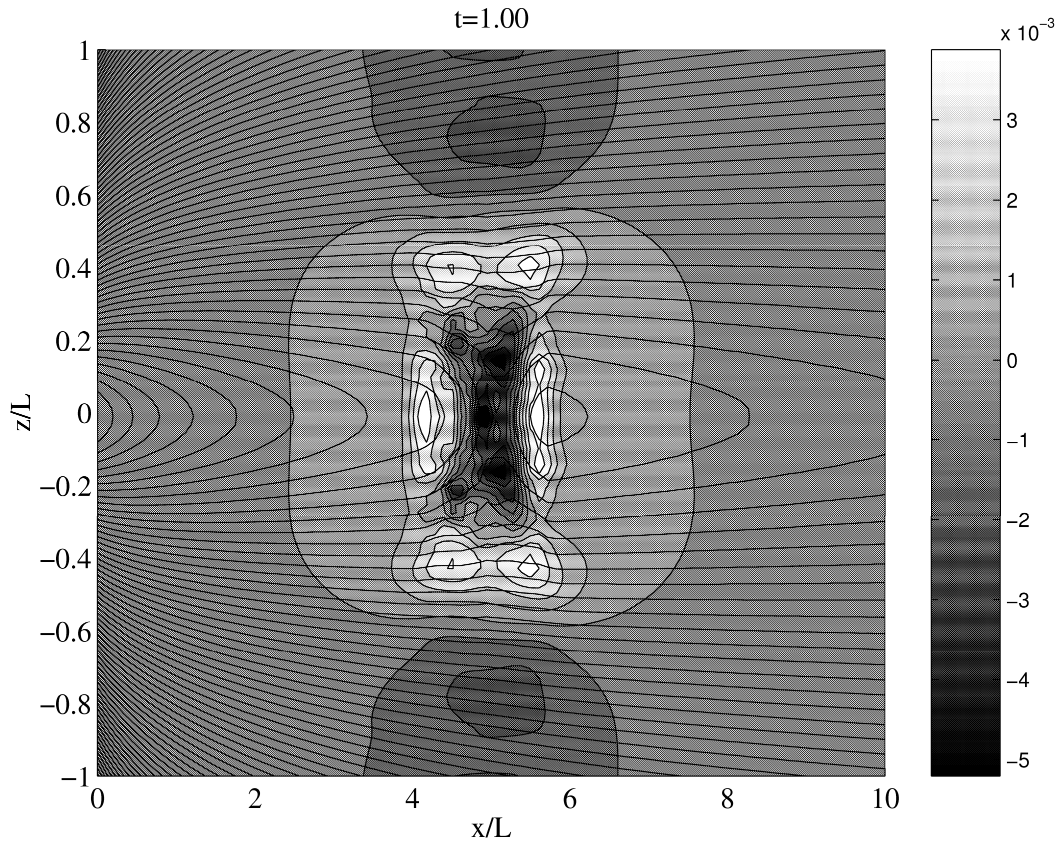

Figure 7: Contours of the vector potential and plasma density variation at time $t = 1.00\tau$.